AD-A079 284 BROWN UNIV PROVIDENCE R I ENGINEERING MATERIALS RESE--ETC F/G 11/6
CREEP OF 2618 ALUMINUM UNDER SIDE STEPS OF TENSION AND TORSION --ETC(U)
AUG 79 W N FINDLEY , J S LAI DAAG29-78-G-0185
UNCLASSIFIED EMRL-72 ARO-15508.2-E NL

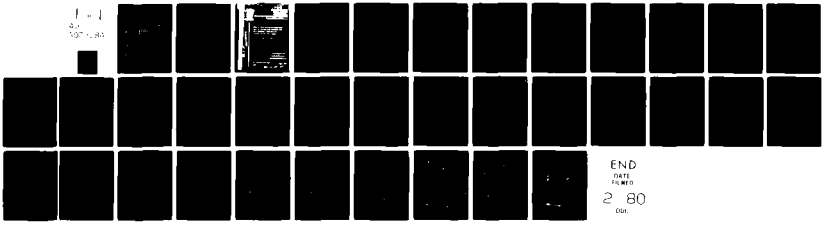

END
DATE FILMED
2 80
DDC

Unclassified

SECURITY CLASSIFICATION OF THIS PAGE (When Data Entered)

REPORT DOCUMENTATION PAGE

READ INSTRUCTIONS BEFORE COMPLETING FORM

1. REPORT NUMBER: (19) 15508.2-E (18) ARO (12)
2. GOVT ACCESSION NO.
3. RECIPIENT'S CATALOG NUMBER

4. TITLE (and Subtitle): (6) Creep of 2618 Aluminum Under Side Steps of Tension and Torsion and Stress Reversal Predicted by a Viscous-Viscoelastic Model
5. TYPE OF REPORT & PERIOD COVERED: (9) Technical Repts
6. PERFORMING ORG. REPORT NUMBER

7. AUTHOR(s): (10) William N. Findley, James S. Lai (12) 36 (15)
8. CONTRACT OR GRANT NUMBER(s): DAAG29-78-G-0185

9. PERFORMING ORGANIZATION NAME AND ADDRESS: Brown University, Providence, Rhode Island 02912 (14) EMRL-72, TR-2
10. PROGRAM ELEMENT, PROJECT, TASK AREA & WORK UNIT NUMBERS

11. CONTROLLING OFFICE NAME AND ADDRESS: U. S. Army Research Office, P. O. Box 12211, Research Triangle Park, NC 27709 (11)
12. REPORT DATE: Aug 79
13. NUMBER OF PAGES: 32

14. MONITORING AGENCY NAME & ADDRESS (if different from Controlling Office)
15. SECURITY CLASS. (of this report): Unclassified
15a. DECLASSIFICATION/DOWNGRADING SCHEDULE

AD A079284

LEVEL II

16. DISTRIBUTION STATEMENT (of this Report)

Approved for public release; distribution unlimited.

DDC DEC 27 1979 RECEIVED

17. DISTRIBUTION STATEMENT (of the abstract entered in Block 20, if different from Report)

DDC FILE COPY

18. SUPPLEMENTARY NOTES

The view, opinions, and/or findings contained in this report are those of the author(s) and should not be construed as an official Department of the Army position, policy, or decision, unless so designated by other documentation.

19. KEY WORDS (Continue on reverse side if necessary and identify by block number)

creep
mathematical models
nonlinear equations
aluminum
stresses
torsion
viscoelasticity
tensile tests

20. ABSTRACT (Continue on reverse side if necessary and identify by block number)

Nonlinear constitutive equations were developed and used to predict the creep behavior of 2618-T61 Aluminum at 200°C (392°F) for combined tension and torsion stresses and under varying stress histories including side step stress changes and stress reversals. The constitutive equations consist of 5 components: linear elastic; time-independent plastic; nonlinear time-dependent recoverable; nonlinear time-dependent nonrecoverable under positive stress; and nonlinear time-dependent nonrecoverable under negative stress. For time-dependent stress inputs, the

DD FORM 1 JAN 73 1473 EDITION OF 1 NOV 65 IS OBSOLETE

Unclassified 405 355

20. ABSTRACT CONTINUED

modified superposition principle and strain hardening are used to describe the behavior of nonlinear time-dependent recoverable and nonlinear time-dependent nonrecoverable respectively. The theory which combines all these features, the viscous-viscoelastic theory, and other modified theories were used to predict from information from constant stress creep the creep behavior of 2618 aluminum under the above stress histories with very satisfactory agreement with the experimental results.

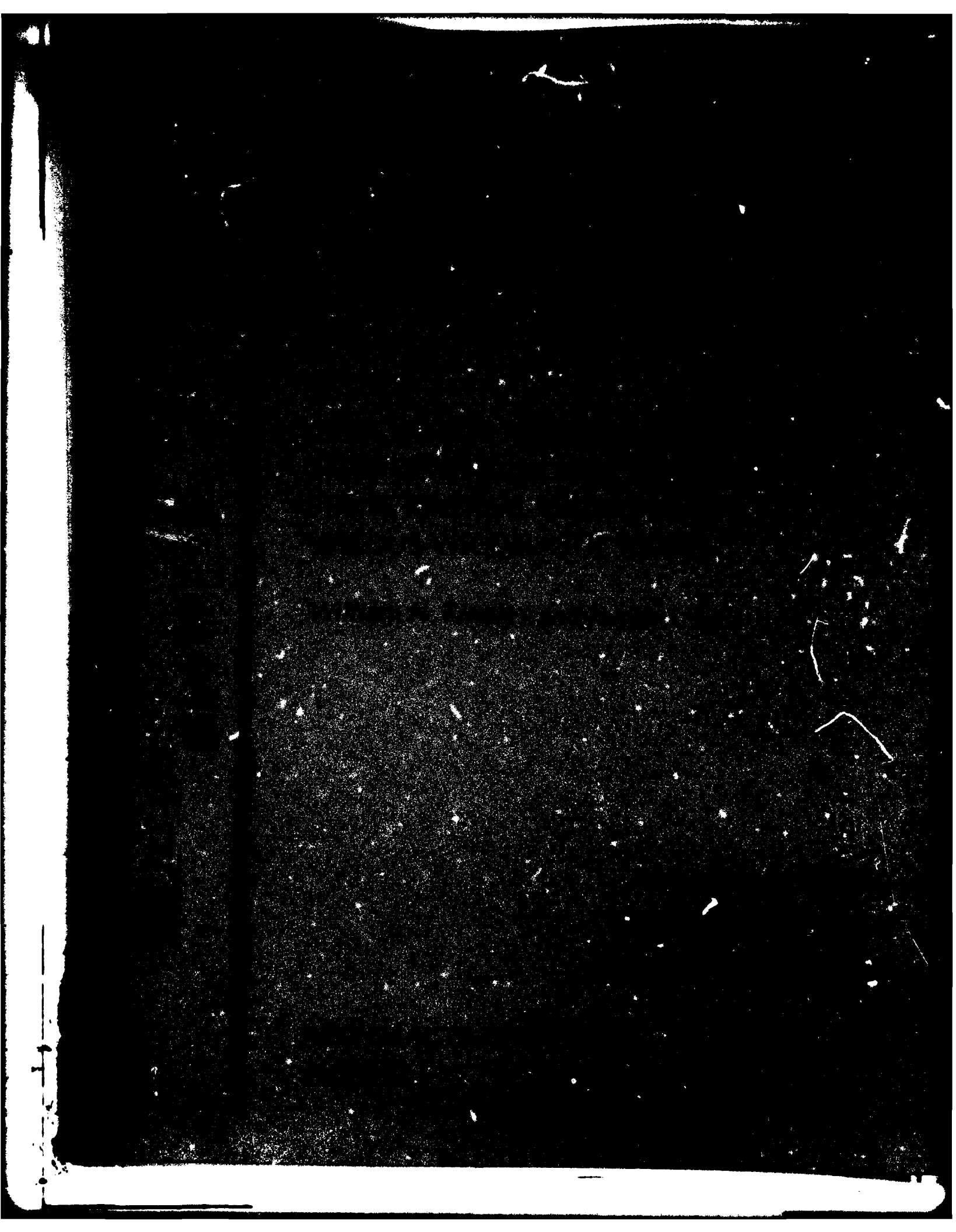

CREEP OF 2618 ALUMINUM UNDER SIDE STEPS OF TENSION AND TORSION AND STRESS REVERSAL PREDICTED BY A VISCOUS-VISCOELASTIC MODEL

by

William N. Findley and James S. Lai

ABSTRACT

Nonlinear constitutive equations were developed and used to predict the creep behavior of 2618-T61 Aluminum at 200°C (392°F) for combined tension and torsion stresses and under varying stress histories including side step stress changes and stress reversals.

The constitutive equations consist of 5 components: linear elastic ε^e ; time-independent plastic ε^p ; nonlinear time-dependent recoverable ε^{ve} ; nonlinear time-dependent nonrecoverable $\varepsilon^v(pos)$ under positive stress; and $\varepsilon^v(neg)$ under negative stress. For time-dependent stress inputs, the modified superposition principle and strain hardening are used to describe the behavior of ε^{ve} and ε^v, respectively. The theory which combines all these features, the viscous-viscoelastic (VV) theory, and other modified (MVV) theories were used to predict from information from constant stress creep the creep behavior of 2618 aluminum under the above stress histories with very satisfactory agreement with the experimental results.

INTRODUCTION

The creep behavior of metals under changing stress--especially changes in state of combined stress and stress reversal--has received little experimental observation. Mathematical expressions employed, such as strain hardening or viscoelastic models, usually are unable to describe the detail of creep behavior under changes such as the above. References to prior work in this area are given in [1].

In a previous paper [1] the authors described a viscous-viscoelastic model in which the strain was resolved into five components: elastic ε^e ; time-independent plastic ε^p ; positive nonrecoverable (viscous) $\varepsilon^v(pos)$; negative nonrecoverable (viscous) $\varepsilon^v(neg)$; and recoverable (viscoelastic) ε^{ve} components. From creep and recovery experiments under combined tension and torsion, the time and stress dependence of these components were evaluated for constant stresses. In [2] constitutive relations for changes in stress state were developed and their predictions were compared with actual creep behavior in simple stress states (uniaxial tension or pure torsion) under step changes in stress.

In the present paper, the constants determined in [1] were used in the same constitutive relations derived in [2], with some additional modifications, to predict the creep behavior of the same material as in [1,2] under combined tension and torsion with time-dependent stress histories including side step changes in tension and torsion and stress reversal in torsion. The last two experiments discussed in the following were reported in [3] as tests E and G.

MATERIAL AND SPECIMENS

An aluminum forging alloy 2618-T61 was employed in these experiments. Specimens were taken from the same lot of 2-1/2 in. diameter forged rod as used in [1,2] and the same lot as specimens D through H in [3]. Specimens were

thin-walled tubes having outside diameter, wall thickness and gage length of 1.00, 0.060 and 4.00 inches, respectively. A more complete description of material and specimens is given in [1].

EXPERIMENTAL APPARATUS AND PROCEDURE

The combined tension and torsion creep machine used for these experiments was described in [4] and briefly in [1]. The temperature control and measurement employed was described in [1,3]. Stress was produced by applying dead weights at the end of levers. The shearing stress and shearing strain reported were computed at mid-wall thickness of the specimen. The gage length employed was measured at room temperature and no correction was made for thermal expansion. The weights were applied by hand at the start of a test by lowering them quickly but without shock. The time of the start of the test was taken to be the instant at which the load was fully applied. In the present experiments changes in loading were made at intervals during the creep tests. The load changes were accomplished by hand in the same manner. Strain was recorded at the following intervals following a load change: every 0.01h to 0.05h; every 0.02h to 0.1h; every 0.05h to 0.5h; every 0.1h to 1.0h; and every 0.2h to 2.0h. All experiments discussed in this paper were performed at 200 ±0.6°C (392°F).

CONSTITUTIVE EQUATIONS FOR CREEP UNDER COMBINED TENSION AND TORSION

In [2] it was shown that creep of 2618 Aluminum at 200°C under combined tension and torsion could be described adequately by the following relation:

$$\varepsilon_{ij}(t) = \varepsilon^{e}_{ij} + \varepsilon^{p}_{ij} + \varepsilon^{v}_{ij}(t) + \varepsilon^{ve}_{ij}(t) \quad , \tag{1}$$

where ε^{e}_{ij} , ε^{v}_{ij} , and ε^{ve}_{ij} represent the time-independent elastic strain, time-dependent nonrecoverable (viscous) strain and time-dependent recoverable (viscoelastic) strain, respectively, and the time-independent plastic strain

ε^p_{ij} was zero in the present experiments. ε^v_{ij} was further resolved into positive and negative parts because of its nonrecoverable feature. Without separate positive and negative parts $\dot{\varepsilon}^v$ would be zero upon stress reversal because it is nonrecoverable. The elastic modulus E_o, shear modulus G_o and Poisson's Ratio ν for the elastic strain component ε^e for the material at 200°C as reported in [1,2] are given in Table I. The constitutive relations for $\varepsilon^v_{ij}(t)$ and $\varepsilon^{ve}_{ij}(t)$ under constant stresses and time-dependent stresses as proposed in [1,2] are reviewed in the following.

Constant Stress

Under constant stress, the components ε^v and ε^{ve} under combined tension σ and torsion τ were represented by the following equations:

$$\varepsilon^{ve}_{11}(t) = \left(\frac{R}{1+R}\right) F\,[(\sigma-\sigma'),(\tau-\tau')]t^n \quad , \tag{2}$$

$$\varepsilon^{ve}_{12}(t) = \left(\frac{R}{1+R}\right) G\,[(\sigma-\sigma'),(\tau-\tau')]t^n \quad , \tag{3}$$

$$\varepsilon^{v}_{11}(t) = \left(\frac{1}{1+R}\right) F\,[(\sigma-\sigma'),(\tau-\tau')]t^n \quad , \tag{4}$$

$$\varepsilon^{v}_{12}(t) = \left(\frac{1}{1+R}\right) G\,[(\sigma-\sigma'),(\tau-\tau')]t^n \quad . \tag{5}$$

The nonlinear functions F and G in (2-5) were derived from a third order multiple integral representation [1,5,6], where for constant stress

$$F(\sigma-\sigma',\tau-\tau') = F_1(\sigma-\sigma') + F_2(\sigma-\sigma')^2 + F_3(\sigma-\sigma')^3 + F_4(\sigma-\sigma')(\tau-\tau')^2 + F_5(\tau-\tau')^2 \tag{6}$$

$$G(\sigma-\sigma',\tau-\tau') = G_1(\tau-\tau') + G_2(\tau-\tau')^3 + G_3(\sigma-\sigma')(\tau-\tau') + G_4(\sigma-\sigma')^2(\tau-\tau') \quad , \tag{7}$$

and σ' , τ' are the components of stress corresponding to a creep limit which may be taken to have a Tresca form defined as follows:

$$(\sigma')^2 + 4(\tau')^2 = (\sigma^*)^2 = (2\tau^*)^2 \quad , \qquad \sigma'/\sigma = \tau'/\tau \quad , \tag{8}$$

and σ^* and τ^* are the creep limits in pure tension and pure torsion, respectively. The coefficients F_i , G_i , and constants σ^* , τ^* , R and n are values determined from constant combined tension-torsion creep tests reported earlier [1] and shown in Table I. The values reported in [1] for F_4 , G_3 and G_4 were incorrect. They should have been as shown in Table I.

Time-Dependent Stress

The modified superposition principle (MSP) derived as a simplification of the multiple integral representation was shown in [2] to describe the time-dependent recoverable (viscoelastic) strain reasonably well. Under a continuously varying stress σ , the strain response ϵ^{ve} under the modified superposition assumption can be represented for nonlinear behavior by

$$\epsilon_{ij}^{ve}(t) = \int_0^t \frac{\partial}{\partial\sigma(\xi)} f_{ij}\,[\bar{\sigma}(\xi),\bar{\tau}(\xi),t-\xi]\;\dot{\bar{\sigma}}(\xi)\;d\xi \quad , \tag{9}$$

where $f_{ij}(\sigma,t)$ represents a nonlinear time-dependent creep function such as (2) and (3) for ϵ_{11}^{ve} and ϵ_{12}^{ve} , respectively, and where $\bar{\sigma}(t) = \sigma(t) - \sigma'(t)$ and $\bar{\tau}(t) = \tau(t) - \tau'(t)$.

For a series of m step changes in stress as employed in the present work, (9) becomes as follows for ϵ_{12}^{ve} for example:

$$\begin{aligned}\epsilon_{12}^{ve}(t) = \left(\frac{R}{1+R}\right)\{&G(\bar{\sigma}_1,\bar{\tau}_1)[t^n-(t-t_1)^n] + \ldots \\ &+ G(\bar{\sigma}_{m-1},\bar{\tau}_{m-1})[(t-t_{m-2})^n-(t-t_{m-1})^n] \\ &+ G(\bar{\sigma}_m,\bar{\tau}_m)(t-t_{m-1})^n\} \quad , \qquad t_{m-1} < t \quad .\end{aligned} \tag{9A}$$

For the time-dependent nonrecoverable (viscous) strain component ϵ^v, it was shown in [2] that the strain hardening theory reasonably represented the behavior of this strain component under a time-dependent stress input. The strain-hardening theory for ϵ^v_{11} and ϵ^v_{12} can be represented by the following equations:

$$\epsilon^v_{11}(t) = \frac{1}{1+R}\left[\int_o^t \{F[\bar{\sigma}(\xi),\bar{\tau}(\xi)]\}^{1/n}\, d\xi\right]^n \quad , \tag{10}$$

$$\epsilon^v_{12}(t) = \frac{1}{1+R}\left[\int_o^t \{G[\bar{\sigma}(\xi),\bar{\tau}(\xi)]\}^{1/n}\, d\xi\right]^n \quad . \tag{11}$$

Equations (10) and (11) were derived from (4) and (5), respectively, using the strain-hardening concept as in [1,2].

For a series of m step changes in stress, as employed in the present paper, (11) for example becomes as follows:

$$\epsilon^v_{12}(t) = \left(\frac{1}{1+R}\right)\{[G(\bar{\sigma}_1,\bar{\tau}_1)]^{1/n}(t_1) + [G(\bar{\sigma}_2,\bar{\tau}_2)]^{1/n}(t_2-t_1) + [G(\bar{\sigma}_3,\bar{\tau}_3)]^{1/n}(t-t_2)\}^n \quad , \quad t_2 < t \quad . \tag{11A}$$

Viscous-Viscoelastic (VV) Theory

The total strain following a time-dependent stress history was found according to (1) by adding to the elastic strain corresponding to the stresses existing at the time of interest the ϵ^{ve} given by (9) and the ϵ^v given by (10) or (11) for axial strain or shear strain.

Modified Viscous-Viscoelastic (MVV) Theory Using σ', τ' (Tresca) Creep Limit

In [2] is was found that the observed characteristics of creep behavior of the material under partial unloading were not properly predicted by the VV theory. It was found, however, that the MVV theory proposed in [2] described the creep behavior of the material under partial unloading

more closely than the VV theory. In the following, the MVV theory, which will be used also in this paper, is reviewed.

The basic difference between the MVV theory and the VV theory is in the treatment of the creep limits for the nonrecoverable strain ϵ^{v} and recoverable strain ϵ^{ve}. It must be noted that every change in combination of stress requires a change in σ', τ' in accordance with (8).

(A) For the nonrecoverable strain component, the strain hardening rule was employed. Upon reduction of stress, the strain rate $\dot{\epsilon}^{v}$ continued at the reduced (increasing) rate prescribed by the strain hardening rule, (10) and (11), until the current stress σ_a equaled or was less than the creep limit, σ'. Under these conditions, when $\sigma_a \leq \sigma'$, $\dot{\epsilon}^{v}$ was zero as prescribed by (10) and (11). Upon reloading to a stress above the creep limit, the nonrecoverable strain rate $\dot{\epsilon}^{v}$ resumed at the rate prescribed by the same equations as though there had been no interval t_x for which $\sigma_a \leq \sigma'$.

(B) For the recoverable strain components ϵ^{ve}, on partial unloading, the recoverable strain rate $\dot{\epsilon}^{ve}$ became and remained zero for all reductions of stress until the total change in stress from the highest stress σ_{max} previously encountered to the current stress σ_a equaled in magnitude the creep limit σ'. That is,

$$\dot{\epsilon}^{ve} = 0 \quad \text{when} \quad (\sigma_{max} - \sigma_a) \leq \sigma' \quad . \tag{12}$$

Equation (12) can be considered as meaning that for a small unloading the recoverable strain component was "frozen" until the stress differential was greater than σ' before the recovery mechanism was activated.

(C) Upon increasing the stress to σ_b $(\sigma_b \geq \sigma_a)$ following a period t_x (a dead zone) for which $(\sigma_{max} - \sigma_a) < \sigma'$ and $\dot{\epsilon}^{ve} = 0$ as discussed in (B) above, the recoverable strain component ϵ^{ve} continues in accordance with the viscoelastic behavior (9) as though the period t_x never occurred. Thus, in computing the behavior for situations described in (B) and (C), it was necessary

to introduce a time shift in equation (9) to eliminate the appropriate period t_x when the ϵ^{ve} was "frozen." Thus, the new time t' subsequent to a period $t_x = (t_b - t_a)$ becomes $t' = t - (t_b - t_a)$, where t is the real time and t_a, t_b are the times when σ_a and σ_b were applied.

(D) In dealing with ϵ^{ve} for <u>decreasing side steps</u>, for example in Fig. 1, period 4, which involved a small decrease in torsion while the tension remained constant, and in period 5 where the tension decreased while the torsion remained constant, the following computations based on the (MVV) theory were used. For ϵ^{ve}_{11} in period 4 of Fig. 1A, the strain components corresponding to σ, σ^2, σ^3, see (6), were considered to continue uninterrupted while the strain corresponding to the terms $\sigma\tau^2$ and τ^2 were considered to remain constant at their values just prior to the stress change. They remained constant because the shear stress change was less than the creep limit. For ϵ^{ve}_{12} in period 4 Fig. 1B, there was no change from the value just preceding the stress change because the $G(\sigma,\tau)$ terms, see (7), decreased and the shear stress decrease was less than the creep limit. Similarly in period 5 Fig. 1 there was no further change in ϵ^{ve}_{11} or ϵ^{ve}_{12}.

(E) In dealing with <u>side steps to zero</u>, such as in period 6, Fig. 1, where one stress component went to zero while the other stress component remained unchanged, ϵ^{ve} was treated in a manner similar to that for decreasing side steps described above. As described later the material behavior suggested that reducing one stress component to zero affected the strains corresponding to mixed stress components as though these components had suffered a small reduction. Considering period 6 of Fig. 1A as an example, ϵ^{ve}_{11} for period 6 was computed by considering that the creep strain components ϵ^{ve}_{11} due to all terms remained constant until both stress components were zero in period 7 at which

time recovery occurred. Recovery of ε_{11} in period 7 was computed as though σ , σ^2 , σ^3 terms recovered from the end of period 4 and $\sigma\tau^2$ and τ^2 terms recovered as from the end of period 3. For ε_{12}^{ve} in period 6, the strain was computed by considering recovery from τ , τ^3 terms as though it started at the end of period 3, while the strain for $\sigma\tau$, $\sigma^2\tau$ terms remained constant. In period 7 recovery continued from τ , τ^3 terms and recovery from the $\sigma\tau$, $\sigma^2\tau$ terms started as though from the end of period 3.

EXPERIMENTAL RESULTS FOR SIDE STEPS AND RECOVERY COMPARED WITH VV AND MVV THEORIES BASED ON TRESCA CREEP LIMIT (σ', τ')

The combined tension and torsion creep experimental results including side steps, recovery and stress reversals are shown in Fig. 1, 2, 3. The VV and MVV theories based on a Tresca form of creep limit (8) were computed for these experiments as described above using the numerical constants obtained from constant stress creep followed by recovery, Table I. Computed creep curves for these theories are shown fully in Fig. 1 only. The predicted behavior for the first 6 periods of Fig. 2 showed similar features as those of Fig. 1 but the creep resulting from the reversals of stress shown in Fig. 2 and 3 was so different from that predicted that a separate treatment was required as discussed in a later section. In Fig. 2 the computed curves for the MVV theory using σ', τ' are shown for periods 3, 4 Fig. 2A and 7, 8 Fig. 2B only to avoid confusion with curves to be discussed later.

In Fig. 1 the predictions of the VV and MVV theories are shown as dot-dot-dash lines and dotted lines respectively. Where the dot-dot-dash line is not shown it is the same as the dotted line.

Figures 1A and 1B show results of a combined tension and torsion experiment in which there was a step increase in tension σ in period 2 with no change in torsion τ . In period 3, there was a step increase in torsion τ ,

with no change in tension σ . This caused a much more marked increase in creep rate than in period 2 for both tension and torsion. Subsequent periods involved partial unloading, first in torsion, then in tension, followed by recovery first in tension, then in torsion. The trend of the data for both components after partial unloading was a small positive (nearly constant) strain rate. The creep rate in tension and torsion decreased considerably in period 4 when the torsion was reduced at a constant tension, but the creep rate in tension was reduced to zero in period 5 when the tension was reduced at a constant torsion. Also there was no change in tensile creep rate in period 6 when the torsion was reduced to zero at a constant tensile stress.

In Fig. 1, the VV theory predicted a somewhat lower rate of creep in period 2 than the test data. In period 3, the actual creep rate was much greater than predicted, especially for ε_{11} . In Fig. 1A period 4, the VV theory showed a slight recovery followed by a positive creep rate whereas there was no indication of recovery in the data. In Fig. 1A, periods 5 and 6, and Fig. 1B, periods 4 and 5, the VV theory predicted a recovery type of decreasing creep rate, whereas the actual data showed a slight but steady increase in strain in both periods. On removal of τ in Fig. 1B, period 6, the shape of the recovery curve for ε_{12} was correctly described. In Fig. 1A period 7, the shape of the predicted recovery of ε_{11} following removal of σ was reasonably well described. However, the new recovery observed in Fig. 1B for period 7 was not predicted by the VV theory.

Computation of the MVV theory for ε_{11}^{ve} for periods 4-7, Fig. 1A, required treating the σ , σ^2 , σ^3 terms separately from the $\sigma\tau$, τ^2 terms because the step-down in τ affected the latter but not the former in period 4. However, ε_{12}^{ve} remained constant for all terms in periods 4 and 5. In periods 6 and 7

all terms of ϵ_{12}^{ve} underwent recovery as though from the end of period 3.

The computed creep curves shown in Fig. 1A and 1B based on the MVV theory were the same as for the VV theory for periods 1-3. They were in good agreement with the test data for periods 4, 5 and 6 in Fig. 1A and periods 4 and 5 in Fig. 1B, except for a vertical displacement caused by the large creep rate in period 3.

The marked difference between the predicted and the observed strains in the third period of Fig. 1 might be a manifestation of material nonlinearity under combined stress not accounted for in the third-order theory. The possibility of employing a fifth-order theory was explored. Additional appropriate higher order terms were added to (6) and (7). This approach did not yield any significant improvement.

As reported in [1] combined tension and torsion tests XI and XII performed at the same stresses yielded a markedly higher creep rate from XI than XII. In [1], Test XI was omitted from the analysis from which the solid lines in Fig. 1 were predicted. Repeating the computations using an average of the results for XI and XII did not yield any overall improvements.

Figures 2A and 2B show the results of the series of changes in stress state during creep for the portion of Test E conducted at 200°C as reported in [3]. In period 1, Fig. 2B, there was pure torsion and in step 2 the torsion was partially unloaded. The observed creep behavior in period 2 showed a nearly constant small positive rate. In period 3, tension was added with no change in torsion. There was only a small increase in the observed torsion creep rate in this period. In period 4 the torsion was removed with no change in the tension. This resulted in essentially no change in tensile creep rate. In period 5, tensile stress was increased and in period 6, the tensile stress was decreased

back to that of period 4. In period 7 negative torsion was added with no change in tension. In period 8, even though tension was removed while torque remained constant there was no change in creep rate in torsion.

The computed creep curves for side steps to zero, periods 6, 7, in Fig. 1 and periods 4, 8 in Fig. 2 showed the same features as the test data except for the following:

(1) The data for recovery of shear strain in periods 6 and 7 of Fig. 1B showed a discontinuity in the recovery when the tensile stress was removed. The viscous-viscoelastic (VV) theory, which employed the Modified Superposition Principle (MSP) simplification, predicted no such discontinuity This may be a deficiency of the MSP simplification. The product form (PF) assumption [6] for the kernel functions in the multiple integral theory is capable of describing such a discontinuity. When the product form assumption was applied to the VV computation of ϵ_{12}^{ve} for Fig. 1B, a discontinuity in the recovery for shear strain was indeed predicted. The discontinuity was much smaller than observed, however.

(2) The observed strain ϵ_{11} in period 6 of Fig. 1A, period 4 of Fig. 2A, period 11 of Fig. 3A, and the ϵ_{12} in period 8 of Fig. 2B continued as though there had been no removal of one of the stress components. The computed value of strain from the VV theory, however, showed a negative rate of creep (recovery).

The discontinuity in recovery in period 7 Fig. 1B was predicted by the MVV theory. This resulted from the fact that recovery associated with the τ , τ^3 terms started at the end of period 5, whereas that associated with the $\sigma\tau$, $\sigma^2\tau$ terms started at the end of period 6.

The computed strain for the MVV theory correctly described the observed behavior of period 6, Fig. 1A, but did not improve (compared to the VV theory)

the prediction of the behavior in the other three instances in which one stress component went to zero while the other remained unchanged. The correct prediction for period 6 Fig. 1A was due to the fact that the removal of τ_1 occurred during a period when σ had previously been reduced so that ε_{11}^{ve} was already constant. The MVV theory assumed that removal of one stress component was equivalent to a small reduction as far as the mixed stress terms were concerned so ε_{11}^{ve} remained constant in period 6.

However, in period 4 of Fig. 2A, period 8 Fig. 2B and period 11 Fig. 3A creep was occurring at the time one stress component was removed. In applying (9A) to this situation for the MVV Theory with σ', τ' (shown in Fig. 2A periods 3, 4, Fig. 2B, periods 7, 8 only) the values of σ' , τ' changed from the previous period to the one in question. This caused the σ , σ^2 , τ^3 terms in periods 3 to 4 Fig. 2A (for example) for ε_{11}^{ve} to predict an apparent recovery even though σ remained constant and the ε_{11}^{ve} for the $\sigma\tau^2$ terms was considered constant.

For period 2 of Fig. 2B the prediction of the VV theory showed a recovery-type behavior, that is, a negative slope of the creep curve with a gradually reducing rate. This was contrary to the observed constant strain during period 2. The shape of the prediction in period 3 was correct. The constant strain in period 2 was correctly predicted by the MVV theory. In period 3 the creep was correctly described by the MVV theory by considering that the strain associated with τ , τ^3 terms was constant and that associated with the mixed terms ($\sigma\tau$,$\sigma^2\tau$) caused creep.

In period 8 of Fig. 2A and period 4 of Fig. 2B the recovery was very well predicted by the MVV theory and the shape correctly predicted by the VV theory. In period 9 of Fig. 2A the torsion was increased while the tension was recovering. This appeared to accelerate the recovery in tension. Similarly, the recovery in torsion in period 5 of Fig. 2B was accelerated by an increase in tension.

The creep resulting from stress reversal in Fig. 2 and 3 will be discussed in a later section.

PREDICTION OF EXPERIMENTS FOR SIDE STEPS AND RECOVERY BY THE VV AND MVV THEORIES BASED ON FIXED CREEP LIMITS IN TENSION σ^* AND TORSION τ^*

It was observed that the discrepancies between the experimental data and the prediction of the MVV theory using the Tresca creep limit resulted from the changes in σ' and τ' that occurred when the state of combined stress changed. These discrepancies were: the apparent recovery type behavior in period 4 Fig. 2A, period 8 Fig. 2B and period 11 Fig. 3a; and the fact that computations for simultaneous torsion creep and tensile relaxation experiments, to be reported later, showed a reversal of the relaxation (increasing strain) under tensile strain when the torsion was reduced to zero. Such a reversal was not observed in the data, but resulted in the computed curves from the change in σ' , τ' .

Accordingly, the apparent creep limit was redefined as fixed values σ^* , τ^* for tensile components and torsion components of stress, respectively, in combined tension and torsion states of stress. It appeared that such a change would improve the prediction of creep behavior in period 3 Fig. 1 as well as periods 4, 8 and 11 in Fig. 2A, 2B and 3A, respectively, and the prediction of some periods of simultaneous tensile relaxation and torsion creep to be reported later.

This change required computing new values of F_4^+ , G_3^+ and G_4^+. At this point it was considered that negative values of these constants were unreasonable since the data showed synergistic effects to be positive. Since the straightforward computation yielded a negative G_3^+ the values of G_3^+ and G_4^+ were redetermined, taking $G_3^+ = 0$ in one case and $G_4^+ = 0$ in another, while maintaining σ^* and τ^* constant. Figures 1, 2, 3 were then recomputed. Also considered were the possibilities: that σ^* , τ^* should be used with the pure stress terms and σ' , τ' for mixed stress terms; that σ^* , τ^* be used

in ε^v and σ' , τ' in ε^{ve} ; and that σ' , τ' be used in ε^v and σ^* , τ^* in ε^{ve} .

From this study it was clear that of all possibilities considered σ^* , τ^* for all terms with $G_4^+ = 0$ yielded the best results. The corresponding values of F_4^+ and G_3^+ are shown in Table II.

The predicted creep results for the experiments are shown in Fig. 1-3 using fixed values of σ^* , τ^* and the constants given in Table I except for F_4^+ , F_5^+ , G_3^+ and G_4^+ which are given in Table II. Computations are shown both for the VV theory (given as dot-dash lines in the figures) and for the MVV theory (given as solid lines in the figures).

The MVV theory using σ^* , τ^* , and $G_4^+ = 0$ show very satisfactory predictions of results in Fig. 1 except for period 3 which is considerably improved in Fig. 1A and better in Fig. 1B. It also improved the prediction of behavior in period 4 of Fig. 2A, period 8 of Fig. 2B and period 11 of Fig. 3A. Most of periods 1-6 in Fig. 2 are satisfactorily predicted by the MVV theory. Subsequent periods in Fig. 2 will be discussed in the following section.

STRESS REVERSALS: EXPERIMENTAL RESULTS AND PREDICTIONS

Reversals of torsion were performed as part of experiments shown in Fig. 2 and 3. In Fig. 2 following recovery in torsion in periods 4, 5 and 6 the shearing stress was partially reversed in period 7 to a negative value less than the maximum positive value in period 1, while the tensile stress remained constant at a level less than its maximum. In Fig. 3 the first reversal of torsion was preceded by positive torsion then recovery at zero stress. The good agreement between theory and data for these two periods is of no significance since these data were used in determining the constants in Table I. In periods 3, 4, and 5 stress reversals were performed in pure torsion. In period 6 a partial stress

reversal occurred and in period 7 tension was added at constant torsion. Periods 8, 9 and 10 included stress reversals in torsion while the tension remained constant.

Straightforward application of the concepts that a portion of the creep of metals is nonrecoverable and strain hardening suggests that reversal of stress would have no effect on the nonrecoverable ε^v component of strain. The fact that an effect was observed was the reason that ε^v was recolved into two parts ε^v_{pos} and ε^v_{neg} in the present investigation. It was considered that positive and negative stresses would produce independent creep responses, the sum of which would be the resulting creep. Thus the shape of a creep curve resulting from complete reversal of stress would be nearly the same as that of the prior positive stressing. It would be the same if all creep was of the nonrecoverable type, but there would be a small difference in the shape of the recoverable creep, in accordance with (9).

An examination of Fig. 3B shows that some of the features expected from the above were realized. Creep in periods 3, 4 and 5, involving reversals of the same stress magnitude showed similar shapes of primary-type creep, although at somewhat higher creep rates at each reversal. The curves for periods 7 and 8 were nearly identical.

However, strain hardening suggests that the creep rate for period 5, taken as the independent effect of the stressing in periods 3 and 5 only, would be much less than that in period 3, which was not as observed. Also the magnitude of creep in period 4 would be much less than that in period 3. That is, it would be shifted by the magnitude of the nonrecoverable creep in period 3. This also was not observed. There was essentially no shift of the required magnitude in periods 3, 4 and 5 or periods 8 and 10. The apparent shift in period 9 is inconsistent. Thus it appeared that the nonrecoverable strain ε^v accumulated prior to reversal of stress was entirely wiped out on completely reversing the stress.

In Fig. 3B the dot-dash lines were computed using the VV theory with Table II and considering all prior strain wiped out upon reversal of stress. The solid lines (MVV theory) were computed considering that the nonrecoverable strain only was wiped out upon reversal of stress and the recoverable strain was computed in the usual manner, by Eq. 9A. Figure 3B shows that the solid lines describe the character of the observed creep for complete stress reversal very well for periods 3, 4, 5 and a shift in period 9.

The dotted lines in periods 6 and 7, for which there was a partial reversal of stress, were computed by not wiping out the nonrecoverable strain at the end of period 6. The difference between the solid and dotted lines in periods 6 and 7 indicate the magnitude of the strain wiped out in arriving at the solid line.

Comparing the solid and dotted lines with the test data for periods 6 and 7 suggests that the nonrecoverable strain was not wiped out at the start of period 6 (which was an incomplete stress reversal). It also suggests that during periods 6 and 7 the prior nonrecoverable strain was gradually wiped out, resulting in the increased rate shown.

The fact that the creep rate in period 5 for example was not reduced as would be expected from strain hardening as a result of the prior negatively stressed period 3 is probably due to the fact that the prior nonrecoverable strain was in fact wiped out (i.e., recovered). Thus there was no residual strain and hence no strain hardening.

The recovery in periods 11 and 12 was computed in the same manner as described in the previous section, with excellent results.

In Fig. 2B there was a reversal of torsion in period 7 during a period of constant, but reduced tensile stress. Both the VV and MVV theories are shown in Fig. 2B. The computations are shown two ways: including the nonrecoverable strain at the end of period 6, as shown by dotted lines; and considering it to

have been wiped out, as shown by solid lines. The torsion in period 7 was not completely reversed. Again, as in period 6 of Fig. 3B, the creep behavior in period 7 Fig. 2B suggested that the residual strain from period 6 was not wiped out during partial reversal of stress but was gradually wiped out during periods 7 and 8 resulting in an increased creep rate. Thus the actual creep started at the dotted line and moved toward the solid line in period 7 Fig. 2B. In period 9 the torsion was increased so that it was then fully reversed. Figure 2B shows both the VV and MVV theories for period 9 with the residual strain wiped out. Also shown as a dotted line is the MVV theory with the residual strain not wiped out. It appears that the actual data continued in period 9 to complete wiping out the residual strain by the end of period 9.

Except for residual strain discussed above the computations for period 8 Fig. 2B were as follows. ε^{v} and ε^{ve} creep associated with τ, τ^3 continued, that associated with $\sigma\tau$, $\sigma^2\tau$ remained constant.

In Fig. 3A, period 7, tension was added to the torsion existing in period 6; and in periods 8, 9 and 10, the torsion was reversed in each period while leaving the tensile stress unchanged. The observed tensile strain ε_{11} in these periods showed a nearly continuous creep with small primary-type responses superimposed at each reversal of torsion as shown by the data in Fig. 3A. Two different computations were made as shown in Fig. 3A. In the first approach, the VV theory (9) and (10) were used to treat the stress states in periods 7 through 11. Since ε_{11} is an even function of τ, changing the stress state from $(\sigma=\sigma_1,\tau=\tau_3)$ to $(\sigma=\sigma_1,\tau=-\tau_3)$ was equivalent to a continuous stressing of $\sigma=\sigma_1$, $\tau=\tau_3$ as far as ε_{11} was concerned. This approach yielded a continuous creep of ε_{11} in periods 7, 8, 9 and 10, as shown by the dot-dash lines in Fig. 3A. Clearly this is an inadequate description of the behavior except for period 7.

Observing that on reversal of shear (torsion) stress in the presence of tension the principal stresses changed direction markedly it was likely that a different set of active elements (slip planes and dislocations) might be involved for positive versus negative shear stress. Thus virgin-type behavior of ε^v might be involved in the axial strain resulting from the first reversal of stress as also observed for the corresponding shear strain component in Fig. 3B. In subsequent reversals only the mixed stress terms were involved in ε^v .

Thus creep for periods 7 through 10 Fig. 3A was computed as follows: The ε^{ve} creep was taken to be continuous since τ appeared as an even power in (6). All stress terms σ , σ^2 , σ^3 , $\sigma\tau^2$ contributed virgin type creep in period 7. The portion of ε^v due to the stressing associated with σ, σ^2 , σ^3 terms in period 7 was taken to be continuous from the beginning of period 7 in subsequent periods. The portion of ε^v due to $\sigma\tau^2$ for positive τ in period 7 remained constant when positive τ was zero in period 8. In period 8 the new negative τ in conjunction with σ caused an additional new virgin-type ε^v creep to be added in period 8. In subsequent periods this new ε^v creep associated with σ , σ^2 , σ^3 was continuous from the start of period 8. In period 9 the new creep associated with $\sigma\tau^2$ from period 8 remained constant and a new virgin-type creep associated with $\sigma\tau^2$ for period 9 was added to the continuing creep from ε^{ve} and the two portions of ε^v associated with σ , σ^2 , σ^3 which were continuous from periods 7 and 8. In a similar manner creep in period 10 consisted of the three continuous creep components plus the sum of the terminal values of $\sigma\tau^2$ creep for each prior interval plus new virgin ε^v creep associated with $\sigma\tau^2$ for period 10. The results as shown in Fig. 3A for the MVV theory, represented by a solid line, are very satisfactory, except that the strain predicted at the start of period 8 was too small.

Another possibility is shown in Fig. 3A by dotted lines, MMVV theory. These curves were computed in the same manner as the solid line except that it was considered that the first reversal of τ (in period 8) resulted in a new virgin ε^{ve} creep (associated with the negative τ) added to the existing ε^{ve} and continuous until periods 11 and 12. In periods 11 and 12 this component was treated the same as the ε^{ve} associated with positive τ . The treatment of the dotted lines in Fig. 3A was similar to that shown as dot-dash lines in Fig. 3B where both ε^{ve} and ε^{v} were considered as new virgin creep at each stress reversal. Fig. 3A shows that the addition of the second ε^{ve} creep in period 8 accounted for most of the step-up in strain in period 8 but resulted in too large a creep rate in period 8 and too rapid recovery in period 12. A comparison of these computed creep curves with the data in Fig. 3A and 3B suggests that the MVV theory shown by the solid lines is the best representation.

Computations for periods 11 and 12 Fig. 3 (for VV and MVV theories) were as follows. In period 11 Fig. 3A, ε^{ve} and ε^{v} creep associated with σ , σ^2 , σ^3 continued while that for $\sigma\tau^2$ remained constant. In period 12 Fig. 3A ε^{v} remained constant, ε^{ve} associated with σ , σ^2 , σ^3 recovered as from the end of period 11 and ε^{ve} associated with $\sigma\tau^2$ recovered as though from the end of period 10. In period 11 Fig. 3B, ε^{v} remained constant, ε^{ve} associated with τ , τ^3 recovered as from the end of period 10 and ε^{ve} associated with $\sigma\tau$, $\sigma^2\tau$ remained constant. In period 12 Fig. 3B ε^{ve} associated with τ , τ^3 continued to recover and ε^{ve} associated with $\sigma\tau$, $\sigma^2\tau$ recovered as though from the end of period 10. This produced the slight step in the MVV Theory between periods 11 and 12 as also observed in the data.

RESULTS AND CONCLUSIONS

Analysis of results of nonlinear creep of 2618 aluminum under combined tension and torsion stress states and under varying stress history including step changes of one stress component while another component remained constant and reversal of shearing stress showed that the viscous-viscoelastic (VV) theory with certain modifications (MVV) theory predicted most of the features of the observed creep behavior quite well.

Among the conclusions are the following:

1. The behavior may be represented by resolving the time-dependent strain into recoverable and nonrecoverable components having the same time dependence.
2. The material behaved as though there was a creep limit such that only very small creep occurred unless the stress was greater than a limiting value having fixed values σ^* , τ^* for tensile stress and shear stress components, respectively.
3. On partial unloading, the material behaved as though the nonrecoverable strain component ϵ^{v} continued to creep in accordance with strain hardening unless the stress became less than the creep limit; whereas the recoverable strain component ϵ^{ve} remained constant unless the decrease (change) in stress exceeded the magnitude of the creep limit.
4. On reloading following an interval t_x of partial unloading involving no further change in ϵ^{ve} the component ϵ^{ve} resumed creeping as though the interval t_x did not exist.
5. An increase in tension under constant torsion was well represented by the theory but a subsequent increase in torsion at constant tension was not as well represented.
6. Reduction of one stress component while the other remained constant required treating the pure stress and mixed stress terms separately. The strains

associated with the mixed stress terms remained constant, whereas the strain behavior associated with the pure stress remained unchanged.

7. Removal of one of two stress components during creep was observed to have no effect on creep associated with the other stress component. This was partially accounted for by considering that the ε^{ve} strain associated with the mixed stress terms remained constant until both stress components were zero.
8. On partial or complete reversal of stress the nonrecoverable strain component ε^{v} behaved as though the reverse stress was applied to a virgin material.
9. If the stress was partially reversed the prior residual strain resulting from ε^{v} remained. However, if the stress component was completely reversed the residual strain from the nonrecoverable strain component ε^{v} appeared to be completely recovered (wiped out).
10. The axial creep resulting from cycles of reversed torsion in the presence of constant tension consisted of: continuous recoverable creep; plus continuous nonrecoverable creep from the first application of positive torsion and also from the first application of negative torsion associated with pure tension terms only; plus new virgin creep associated with the mixed tension-torsion stress terms at each reversal of torsion.

ACKNOWLEDGMENT

This work was supported by the Office of Naval Research and the Army Research Office, Research Grant No. DAAG29-78-G-0185. The material was contributed by the Aluminum Company of America. The authors are grateful to: U. W. Cho for helpful discussions and recomputation of theory; R. M. Reed for performing one experiment; and M. C. Gingrich for typing the manuscript.

REFERENCES

1. Findley, W. N., and Lai, J. S., "Creep and Recovery of 2618 Aluminum Alloy Under Combined Stress with a Representation by a Viscous-Viscoelastic Model," Trans., ASME, Journal of Applied Mechanics, Vol. 45, September 1978, pp. 507-514.

2. Lai, J. S., and Findley, W. N., "Creep of 2618 Aluminum Under Step Stress Changes Predicted by a Viscous-Viscoelastic Model," EMRL-71, Brown University, April 1979.

3. Blass, J. J., and Findley, W. N., "Short-Time Biaxial Creep of an Aluminum Alloy with Abrupt Changes of Temperature and State of Stresses," Trans., ASME, Journal of Applied Mechanics, Vol. 38, Series E, No. 2, June 1971, pp. 489-501.

4. Findley, W. N., and Gjelsvik, A., "A Biaxial Testing Machine for Plasticity, Creep or Relaxation Under Variable Principal-Stress Ratios," Proc., American Society for Testing and Materials, Vol. 62, 1962, pp. 1103-1118.

5. Green, A. E., and Rivlin, R. S., "The Mechanics of Nonlinear Materials with Memory, Part I," Archive for Rational Mechanics and Analysis, Vol. 1, 1957.

6. Findley, W. N., Lai, J. S., and Onaran, K., Creep and Relaxation of Nonlinear Viscoelastic Materials, North-Holland Publishers, Amsterdam, 1976.

Table I. Constants for Equations (2) through (11) Using σ' , τ' for F_4^+ , G_3^+ and G_4^+

$F_1^+ = 6.084 \times 10^{-12}$, per Pa-$h^n$ (0.004195, % per ksi-h^n)
$F_2^+ = -7.431 \times 10^{-20}$, per Pa^2-h^n (-0.0003533, % per ksi^2-h^n)
$F_3^+ = 7.596 \times 10^{-28}$, per Pa^3-h^n (0.0000249, % per ksi^3-h^n)
$\sigma^* = 9.143 \times 10^7$, Pa (13.26, ksi)
$G_1^+ = 7.170 \times 10^{-12}$, per Pa-$h^n$ (0.004944, % per ksi-h^n)
$G_2^+ = 2.703 \times 10^{-28}$, per Pa^3-h^n (0.00000886, % per ksi^3-h^n)
$\tau^* = 4.571 \times 10^7$, Pa (6.630, ksi)
$F_4^+ = 1.0491 \times 10^{-28}$, per Pa^3-h^n (0.000003439, % per ksi^3-h^n)
$F_5^+ = 0$
$G_3^+ = -4.020 \times 10^{-20}$, per Pa^2-h^n (-0.0001911, % per ksi^2-h^n)
$G_4^+ = 9.222 \times 10^{-28}$, per Pa^3-h^n (0.00003023, % per ksi^3-h^n)

Note: $n = 0.270$
$R = 0.55$
$E_o = 6.5 \times 10^4$MPa (9.43×10^6 psi)
$G_o = 2.45 \times 10^4$MPa (3.57×10^6 psi)
$\nu = 0.321$

Table II. Constants for Equations (2) through (11) Using σ^* , τ^* for F_4^+ and G_3^+

F_1^+ , F_2^+ , F_3^+ , σ^* , G_1^+ , G_2^+ , τ^* , n and R are the same as in Table I.

$F_4^+ = 6.214 \times 10^{-27}$ per $Pa^3\text{-}h^n$ (0.0002037, % per $ksi^3\text{-}h^n$)

$F_5^+ = 0$

$G_3^+ = 1.562 \times 10^{-19}$ per $Pa^2\text{-}h^n$ (0.0007424, % per $ksi^2\text{-}h^n$)

$G_4^+ = 0$

FIGURE CAPTIONS

Fig. 1A. Tensile Strain for Combined Tension and Torsion Creep of 2618-T61 Al at 200°C Under Side-Steps of Loading, Unloading and Recovery. Where the VV theory is not shown it is the same as the MVV theory. Numbers indicate periods on insert.

σ_1 = 119.5 MPa (17.33 ksi),
σ_2 = 143.4 MPa (20.8 ksi),
τ_1 = 69.0 MPa (10 ksi),
τ_2 = 82.7 MPa (12 ksi).

Fig. 1B. Shearing Strain for Combined Tension and Torsion Creep of 2618-T61 Al at 200°C Under Side-Steps of Loading, Unloading and Recovery. Where the VV theory is not shown it is the same as the MVV theory. Numbers indicate periods on insert.

σ_1 = 119.5 MPa (17.33 ksi),
σ_2 = 143.4 MPa (20.8 ksi),
τ_1 = 69.0 MPa (10 ksi),
τ_2 = 82.7 MPa (12 ksi).

Fig. 2A. Tensile Strain for Combined Tension and Torsion Creep of 2618-T61 Al at 200°C Under Side-Steps, Partial and Complete Reversal of Torsion. Where the VV theory is not shown it is the same as the MVV theory. Numbers indicate periods on insert.

σ_1 = 122.0 MPa (17.7 ksi),
σ_2 = 172.4 MPa (25 ksi),
τ_1 = 99.3 MPa (14.4 ksi),
τ_2 = 70.3 MPa (10.2 ksi).

Fig. 2B. Shearing Strain for Combined Tension and Torsion Creep of 2618-T61 Al at 200°C Under Side-Steps, Partial and Complete Reversal of Torsion. Where the VV theory is not shown it is the same as the MVV theory. Numbers indicate periods on insert.

σ_1 = 122.0 MPa (17.7 ksi),
σ_2 = 172.4 MPa (25 ksi),
τ_1 = 99.3 MPa (14.4 ksi),
τ_2 = 70.3 MPa (10.2 ksi).

Fig. 3A. Tensile Strain for Combined Tension and Torsion Creep of 2618-T61 Al at 200°C Under Stress Reversals in Torsion with and without Tensile Stress. Where the VV theory is not shown it is the same as the MVV theory. Numbers indicate periods on insert.

σ_1 = 122.0 MPa (17.7 ksi),
τ_1 = 79.3 MPa (11.5 ksi),
τ_2 = 99.3 MPa (14.4 ksi),
τ_3 = 70.3 MPa (10.2 ksi).

Fig. 3B. Shearing Strain for Combined Tension and Torsion Creep of 2618-T61 Al at 200°C Under Stress Reversals in Torsion with and without Tensile Stress. Where the VV theory is not shown it is the same as the MVV theory. Numbers indicate periods on insert.

σ_1 = 122.0 MPa (17.7 ksi),
τ_1 = 79.3 MPa (11.5 ksi),
τ_2 = 99.3 MPa (14.4 ksi),
τ_3 = 70.3 MPa (10.2 ksi).

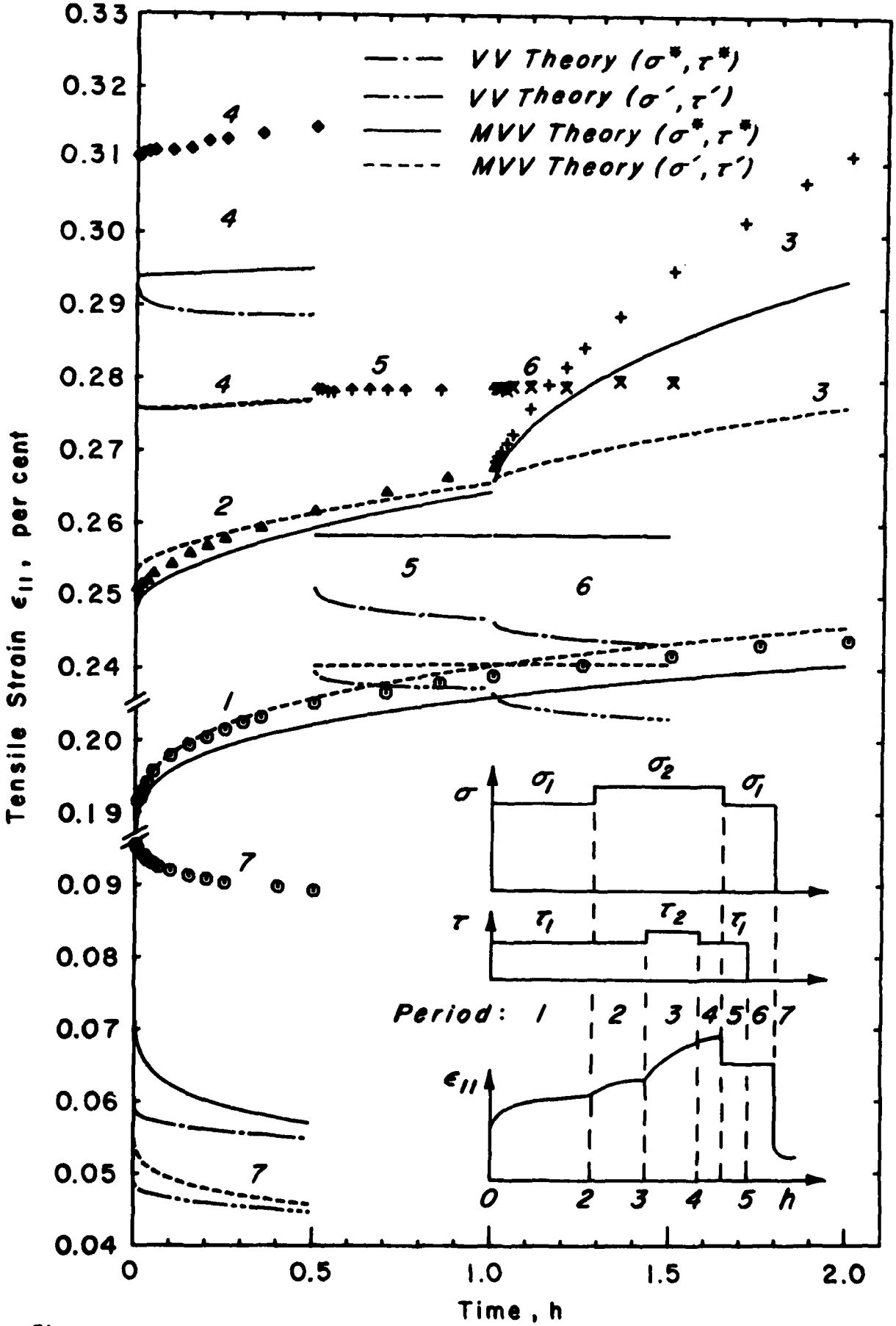
VV Theory (σ*, τ*)
VV Theory (σ′, τ′)
MVV Theory (σ*, τ*)
MVV Theory (σ′, τ′)
Tensile Strain ε11, per cent
Time, h
0.33
0.32
0.31
0.30
0.29
0.28
0.27
0.26
0.25
0.24
0.20
0.19
0.09
0.08
0.07
0.06
0.05
0.04
0
0.5
1.0
1.5
2.0
σ
σ1
σ2
τ
τ1
τ2
Period: 1 2 3 4 5 6 7
ε11
0 2 3 4 5 h

Fig. 1A.

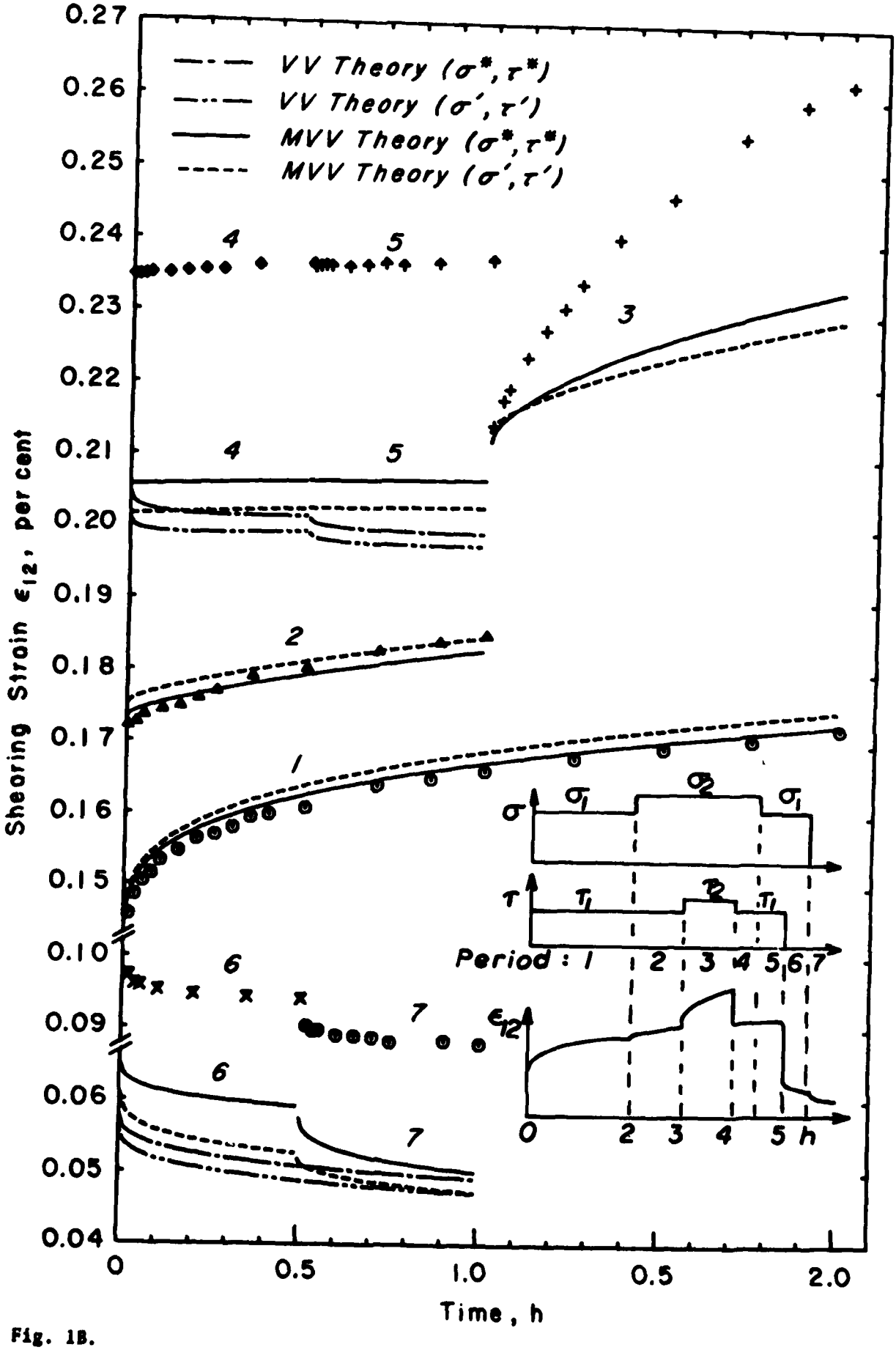
VV Theory (σ*, τ*)
VV Theory (σ', τ')
MVV Theory (σ*, τ*)
MVV Theory (σ', τ')
Shearing Strain ε12, per cent
Time, h
Period : 1 2 3 4 5 6 7
σ
τ
ε12
0 2 3 4 5 h

Fig. 18.

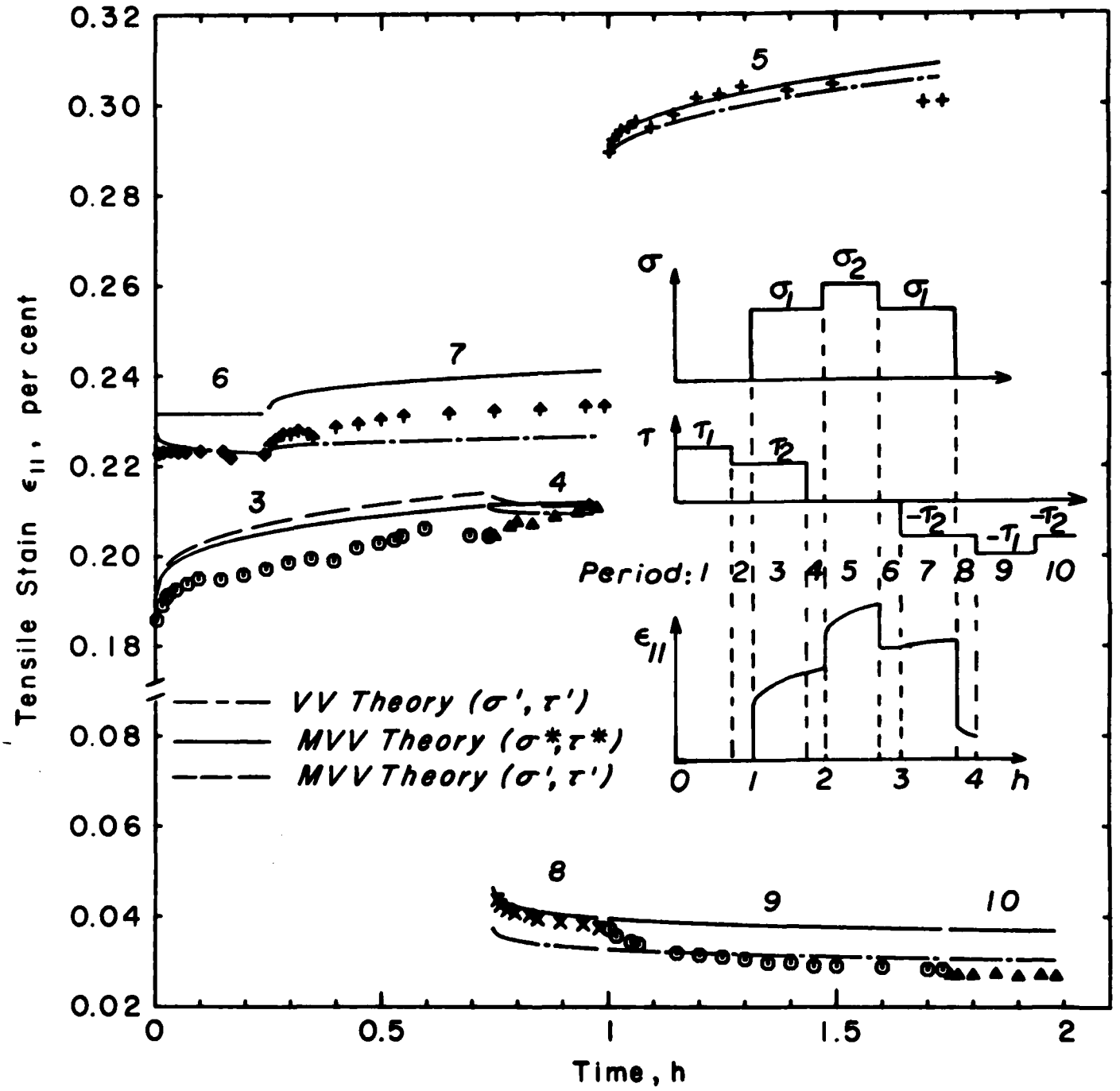
0.32
0.30
0.28
0.26
0.24
0.22
0.20
0.18
0.08
0.06
0.04
0.02
0
0.5
1
1.5
2
Time, h
Tensile Stain ϵ_{11}, per cent
5
6
7
3
4
8
9
10
VV Theory (σ', τ')
MVV Theory (σ*, τ*)
MVV Theory (σ', τ')
σ
σ1
σ2
τ
τ1
τ2
-τ2
-τ1
Period: 1 2 3 4 5 6 7 8 9 10
ϵ_{11}
0 1 2 3 4 h

Fig. 2A.

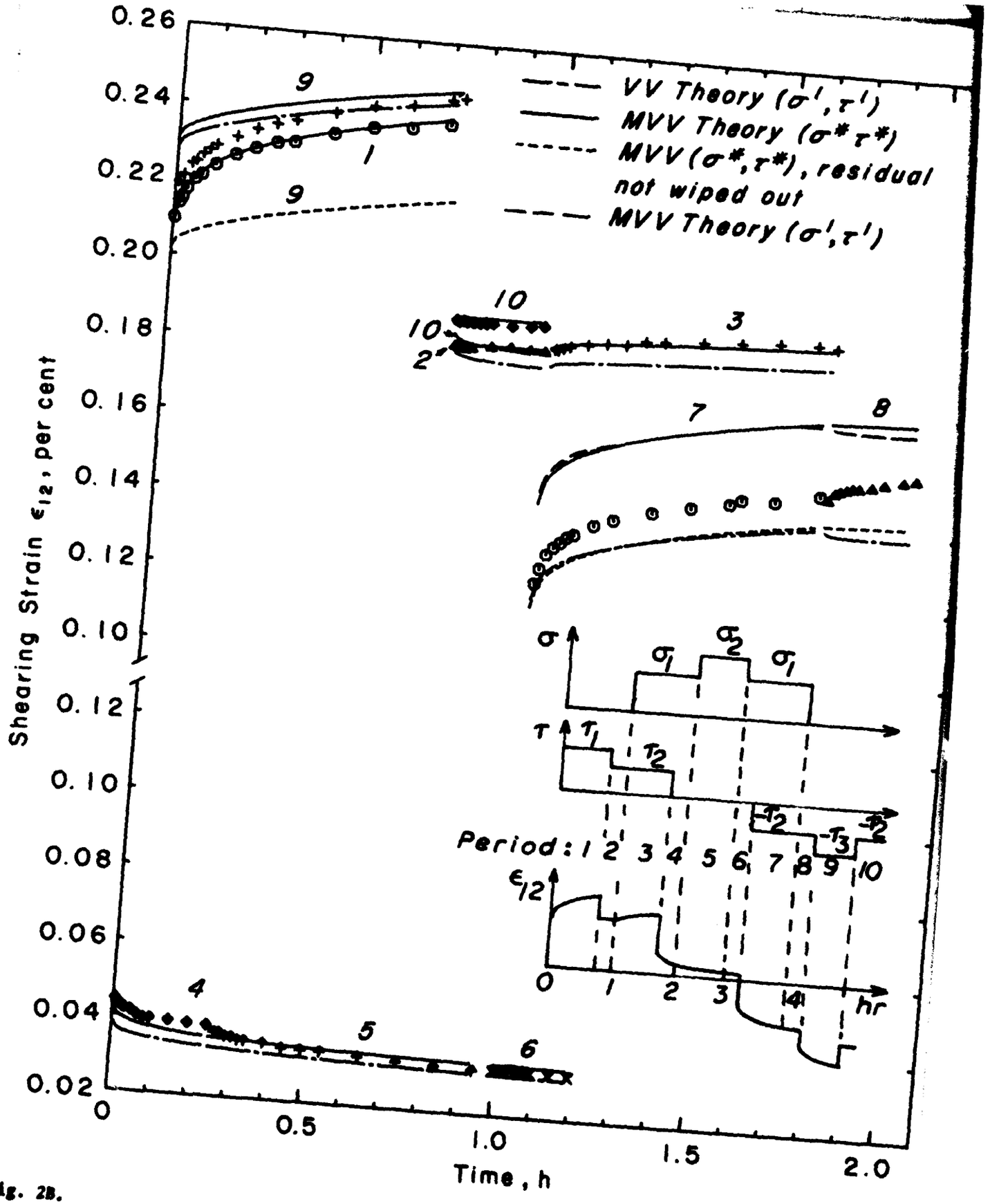
VV Theory (σ', τ')
MVV Theory (σ^* τ^*)
MVV (σ^*, τ^*), residual not wiped out
MVV Theory (σ', τ')
Shearing Strain ϵ_{12}, per cent
Time, h
Period: 1 2 3 4 5 6 7 8 9 10
hr

Fig. 2B.

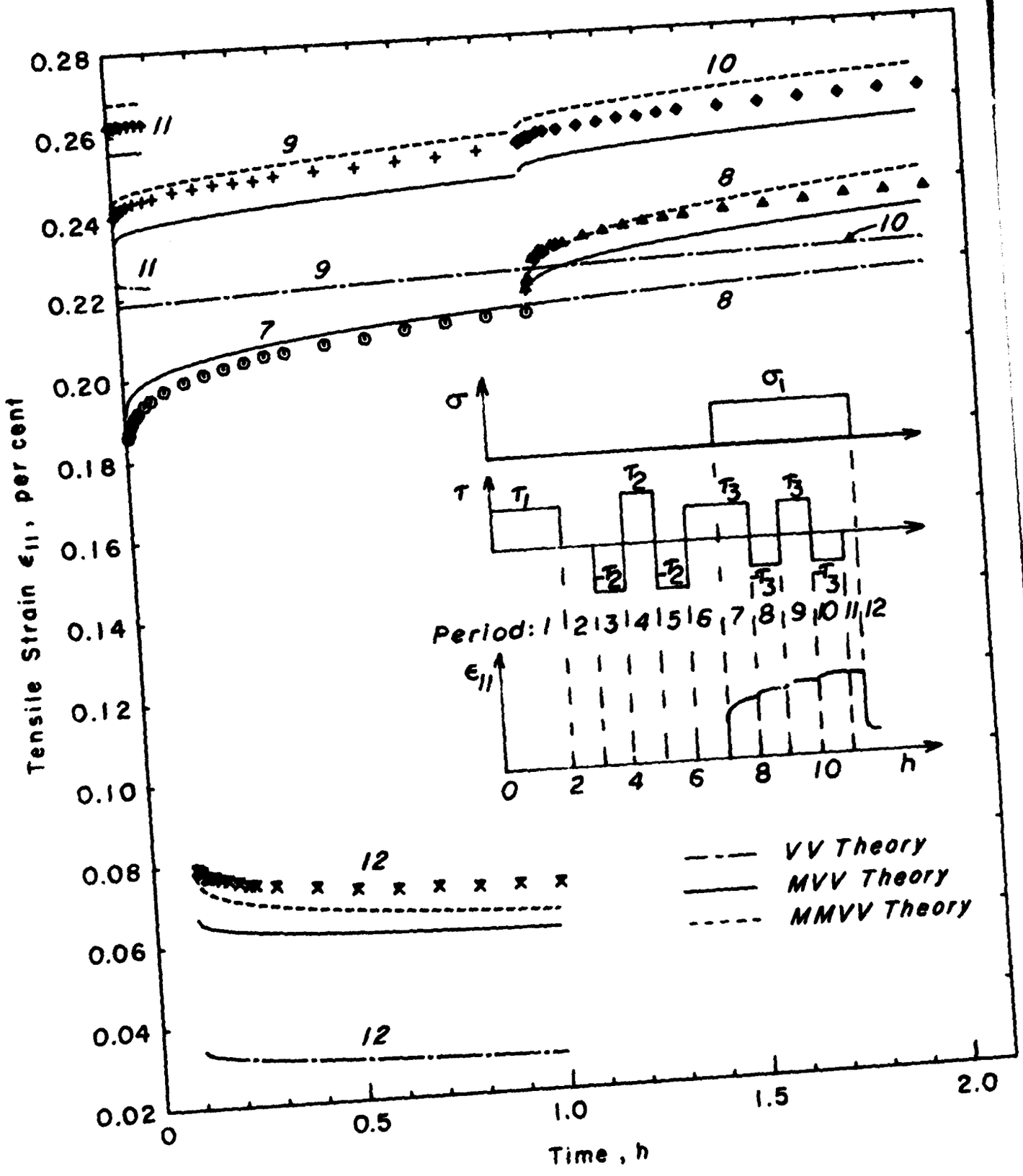
0.28
0.26
0.24
0.22
0.20
0.18
0.16
0.14
0.12
0.10
0.08
0.06
0.04
0.02
0
0.5
1.0
1.5
2.0
Time , h
Tensile Strain ϵ_{11}, per cent
10
11
9
8
7
12
σ
σ_1
τ
τ_1
τ_2
τ_3
Period: 1 2 3 4 5 6 7 8 9 10 11 12
ϵ_{11}
0 2 4 6 8 10 h
VV Theory
MVV Theory
MMVV Theory

Fig. 3A.

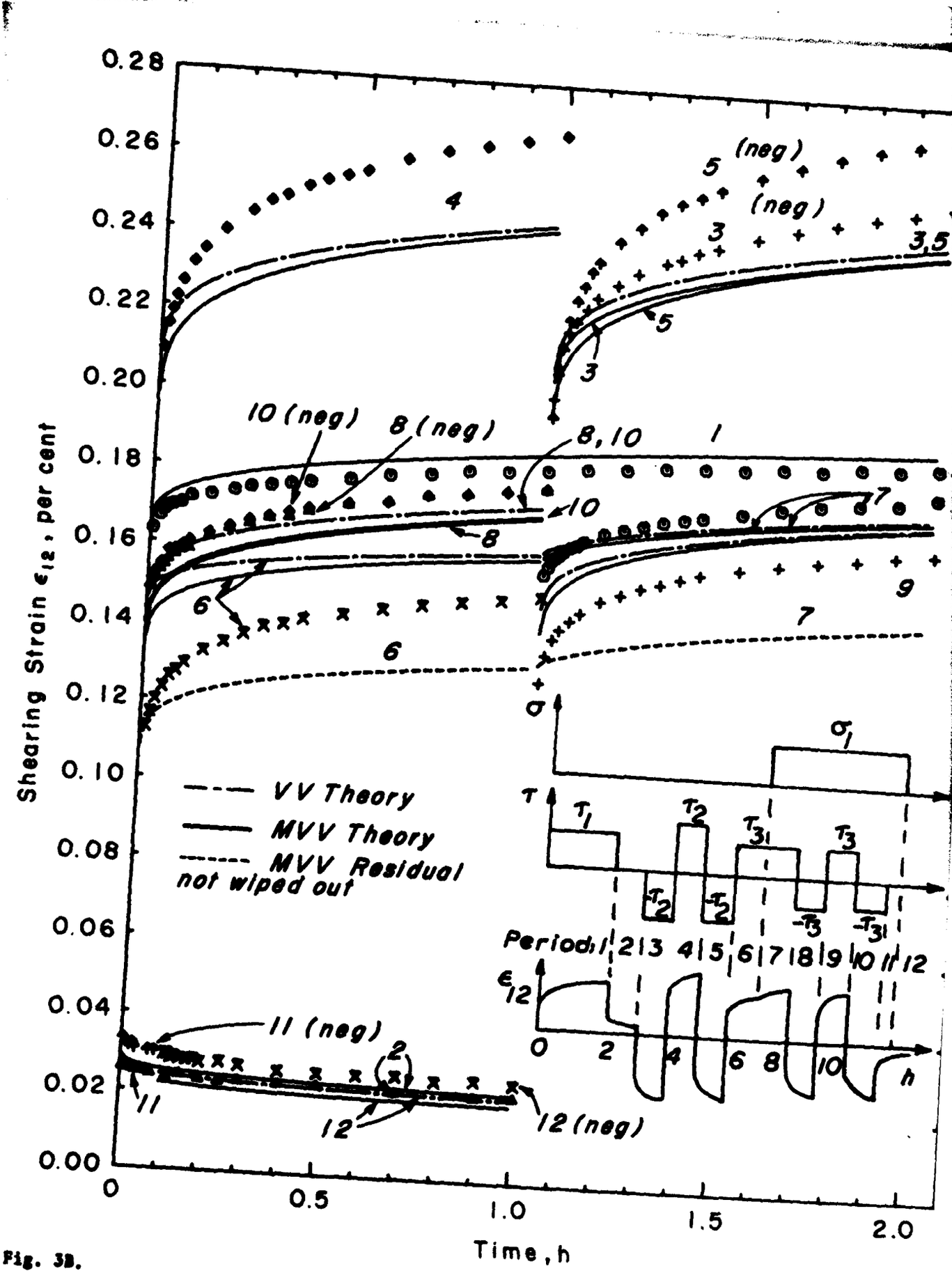
Shearing Strain ϵ_{12}, per cent
Time, h
VV Theory
MVV Theory
MVV Residual not wiped out
4
5 (neg)
3
3,5
5
10 (neg)
8 (neg)
8,10
1
10
8
7
6
9
7
6
11 (neg)
2
11
12
12 (neg)
σ
σ_1
τ
τ_1
τ_2
τ_{31}
τ_3
$-\tau_2$
$-\tau_2$
$-\tau_3$
$-\tau_{31}$
Period, 1 2 3 4 5 6 7 8 9 10 11 12
ϵ_{12}
0 2 4 6 8 10 h

Fig. 3B.